Modelling the effects of confinement on the glass transition temperature and segmental mobility

2003 J. Phys.: Condens. Matter 15 S1019

(http://iopscience.iop.org/0953-8984/15/11/324)

INSTITUTE OF PHYSICS PUBLISHING JOURNAL OF PHYSICS: CONDENSED MATTER

J. Phys.: Condens. Matter **15** (2003) S1019–S1029 PII: S0953-8984(03)56902-8

Modelling the effects of confinement on the glass transition temperature and segmental mobility

D Kranbuehl, R Knowles, A Hossain and M Hurt

Chemistry Department, College of William and Mary, Williamsburg, VA 23187, USA

Received 27 September 2002, in final form 25 November 2002
Published 10 March 2003
Online at stacks.iop.org/JPhysCM/15/S1019

Abstract

An off-lattice simulation of the effect of confinement geometry on segmental mobility and the glass transition temperature has been conducted using Monte Carlo techniques. The off-lattice random coil Monte Carlo model represents the polymer chains, $N - 1$ units long, as a string of N impenetrable spheres. The segmental mobility is characterized by monitoring the mean square displacement of a bead over two different time intervals, one and fifty Rouse relaxation times, as the temperature is lowered. The change in volume fraction of occupied space, a measure of density, is monitored to detect the glass transition temperature T_g. Simulations have been conducted on freely jointed polymer chains, which have been spatially confined by one dimension (between parallel plates) and by three dimensions (in a sphere).

For both environments the value of T_g decreases as the confining dimension decreases in length. The onset of the decrease occurs first when the confinement is 3D and the magnitude of the effect is largest for 3D confinement. For 3D spherical confinement, throughout the cooling cycle, the segmental beads have a significantly higher mobility in the outer spherical region compared to those near the centre of the confinement space. For the 1D confinement, between two plates, any differences in mobility for regions near the plates compared to the centre region disappear as the temperature is lowered.

(Some figures in this article are in colour only in the electronic version)

1. Introduction

Over the past decade, a significant amount of research has focused on the pioneering results of Jackson and McKenna [1, 2] that showed the value of the glass transition temperature is lowered when small glass forming molecules are confined in pores with nano dimensions. Many reports using a variety of techniques including dielectric relaxation, NMR, neutron spectroscopy and time-resolved optical techniques have shown that spatial confinement of molecules in cavities with nano dimensions does affect the glass transition temperature [3–33].

Two major physical effects have been observed and discussed. One is the effect on molecular motion due to the high surface area relative to the volume of the relaxing molecules. The second is the dynamic behaviour of the molecules in the centre of the confining walls. The effect of the surface is highly dependent on whether there are attractive forces between the confining walls and the confined liquid or whether these attractive interactions are absent, resulting in repulsive forces. In the former case, the dynamic mobility near the wall is decreased and when the attractions are strong the value of T_g is actually increased.

The behaviour of the molecules in the presence of a purely repulsive interaction at the wall is more complex. Overall, most experimental results show that in this case the glass transition temperature is decreased and that the molecules experience an increase in their mobility. This has been explained by viewing the walls as limiting the cooperative length scale of the α-relaxation glass transition process and thereby increasing the mobility while decreasing the glass transition temperature [5, 17, 32, 33]. A more detailed physical picture has been proposed which interprets the dynamic behaviour as observed experimentally in terms of a three-layer model of increasing mobility towards the pore centres [12].

Theoretical Monte Carlo model studies have also been conducted which show the effect of a confining environment [17, 28–31]. In another Monte Carlo study, the effect of a purely repulsive constraining wall was shown to decrease the value of T_g [32]. Here the effect occurred first in 3D confining spheres and at a much smaller confining distance in 1D confinement between parallel plates. These results were in agreement with experimental dielectric results on a system where the dimensionality of the confinement was varied [27].

The purpose of this paper is to examine the effect of confinement on the segmental mobility of the polymer chains and on the mobility of the chain's centre of mass. Here we examine the variation in mobility from the centre of the confining space to the outer region near the confining walls under a purely repulsive interaction with the wall. Monte Carlo model studies are reported on the distance moved per unit time for 10-bead polymer chains in spherical 3D and parallel plate 1D confinement. For each environment the mobility of individual beads and the centre of mass is monitored.

2. Simulation model

In our off-lattice random-coil Monte Carlo model, a single polymer chain $N - 1$ units long is modelled by a string of N impenetrable beads [34, 35]. The beads are of unit diameter, touching spheres (see figure 1). The vectors connecting bead centres along the chain are each one unit in length. Each bead vector pair is taken to represent one 'statistical segment', i.e. a moderately large number of chemical monomers in a real polymer chain. No restriction is placed on the angle between successive beads connecting vectors along the chain. Brownian motion of a real chain is represented by sequences of elementary moves we call 'move cycles'. Each move cycle consists of selecting a single bead of the chain at random and attempting a local move of that bead and its connecting vectors. The attempted move is to a position obtained by rotating the selected bead about an axis passing through the centres of its immediate neighbours along the chain, through an angle chosen at random in the range $(-\pi, \pi)$ (see figure 1). For an end bead, with only one neighbour, the rules are modified by first generating the centre coordinate of a 'phantom' bead at unit distance and randomly chosen direction from the selected end bead. The potential energy function is a hard-sphere repulsion of the bead radius, r (excluded volume), a finite attractive potential V/kT between r and $r + 1.0$ and zero for larger distances between beads. The decision to move or not to move the chosen bead is determined by calculating the difference ΔE between the selected bead and all the other beads before and after the proposed

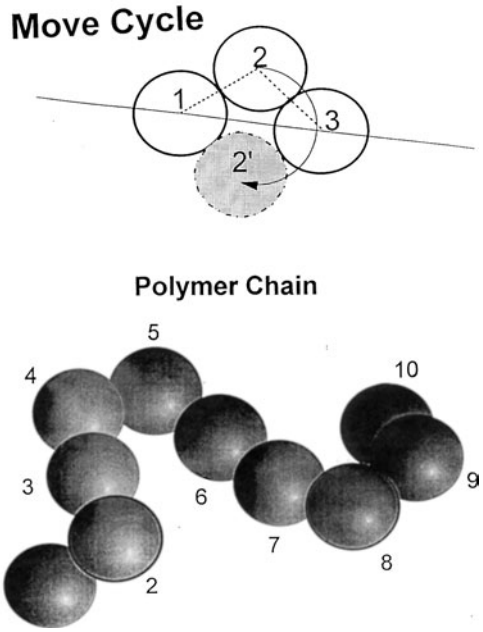

Figure 1. Move cycle and picture of a 10-bead polymer chain.

move; then moving it with a probability p where $\Delta E = V/kT$ (final) $-V/kT$ (initial) and

$$p = \begin{cases} 1 & \text{if } \Delta E < 0 \\ \exp(-\Delta E) & \text{if } \Delta E > 0. \end{cases}$$

In the present study, freely jointed statistical segment polymer chains with 10 hard sphere beads were studied in two types of constraining environments with purely repulsive walls; in spheres, and between plates representing constraint conditions of three and one dimension (3D and 1D, respectively). These environments and the various constraint lengths are reported in table 1. The non-constraining dimension of the 1D plates was three or more multiples of the constraining plate separation.

Nine independent equilibrium configurations were obtained for each environment with interaction-temperature–potential value of $V/kT = 0.0$. That is, the attractive potential well was zero at the equilibrium. Each of the nine equilibrium configurations for each environment was generated by running the simulation once in equilibrium for an additional time, estimated to be at least ten times the limiting Rouse relaxation time, a relaxation time proportional to $(N-1)^{2.2}$, where $N-1$ is the number of statistical segments in the chain [34, 35]. The quench was then simulated by increasing the value of V/kT at rates designated as $0.1x$ and x. A quench speed of $0.1x$ represents approximately 200 Rouse relaxation times during the course of a quench from 0 to -2.0. Thus, $0.1x$ is equivalent to one Rouse relaxation time per $0.01\ V/kT$ change in temperature. As the value of V/kT is increased or the temperature is lowered at a constant rate per move, 'a cycle', the well becomes more attractive. This attraction draws the beads closer together, decreasing the volume and the mobility of the chain beads. Eventually, this decrease in volume or increase in density, as measured by volume fraction of occupied space, is so great that the beads or molecules become locked up to form a material in which the volume change with temperature is much less (i.e. a glass).

Table 1. Values of T_g for each environment and cooling rate (R, radius; D, constraint and confining distance; H, height and thickness of film).

System	D Constraint	$1/T_g$	T_g	Cooling rate
Sphere $R = 8$	16	0.51	1.96	$1/10x$
	3D	0.5	2	$1x$
Sphere $R = 6$	12	0.47	2.12	$1/10x$
	3D	0.5	2	$1x$
Sphere $R = 4$	8	0.89	1.12	$1/10x$
	3D	0.84	1.19	$1x$
Sphere $R = 3$	6	0.96	1.04	$1/10x$
	3D	0.93	1.075	$1x$
Film $H = 12$	12	0.65	1.54	$1/10x$
	1D	0.56	1.79	$1x$
Film $H = 8$	8	0.44	2.27	$1/10x$
	1D	0.44	2.27	$1x$
Film $H = 6$	6	0.84	1.19	$1/10x$
	1D	0.74	1.35	$1x$
Film $H = 3$	3	0.91	1.1	$1/10x$
	1D	0.85	1.18	$1x$
Film $H = 2$	2	1.04	0.96	$1/10x$
	1D	1.24	0.81	$1x$

The volume fraction of occupied space was monitored by monitoring the amount of space occupied by beads in a region located in the centre of the confining environment. The density was calculated by dividing the amount of space occupied by beads and the fraction of beads lying within the sampling space by the volume of the sampling space. The volume of this region for calculating changes in volume fraction of occupied space was, in general, about 0.3 of the total volume. In all cases, the effect of cooling was to uniformly pull the beads together away from the repulsive wall with no apparent spatial heterogeneity. The effective density, as reported here, is approximately half the density in units of g cm^{-3} of hydrocarbons based on using their van der Waal volumes to estimate their volume fraction of occupied space. Thus, a starting volume fraction density of 0.24 (as seen in figure 2) represents an approximate hydrocarbon density of 0.48 g cm^{-3}.

3. Results

The nine independent starting configurations for each environment listed in table 1 were quenched at two rates of cooling and the volume fractions of occupied space, our effective density, were averaged for each value of V/kT. As the temperature is lowered by increasing V/kT and thereby the depth of the attractive potential, a distinct transition occurs in the rate of change of the density with V/kT. Figure 2 shows for a 3D constraining environment the variation in the density versus the two rates of change in $\Delta E = V/kT$. Simulations were run at higher densities of 0.32, representing an approximate hydrocarbon density of 0.64 g cm^{-3} for 10-bead chains and for longer 20-bead chains.

Both increasing the density and increasing the polymer length produced results similar to those in figure 2; that is, a distinct transition from liquid-like to glass-like behaviour in the rate

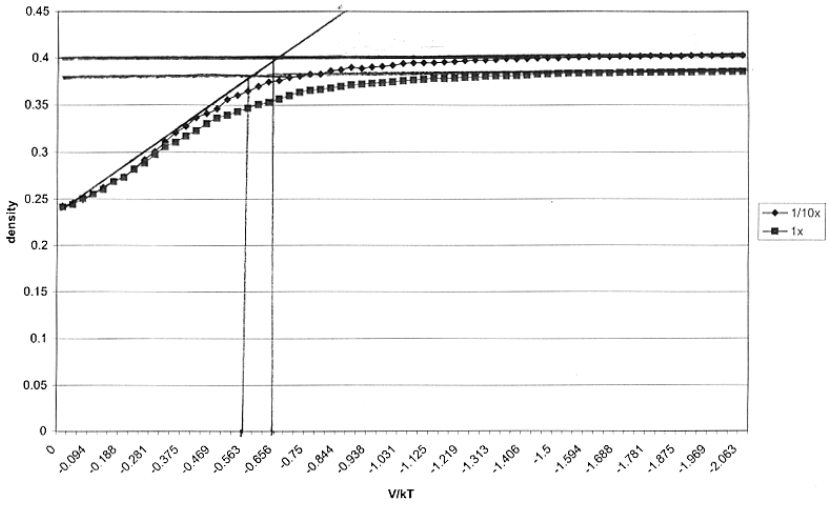

Figure 2. Change in density with decrease in V/kT at two cooling rates and determination of T_g from intersection of the liquid and glass density lines.

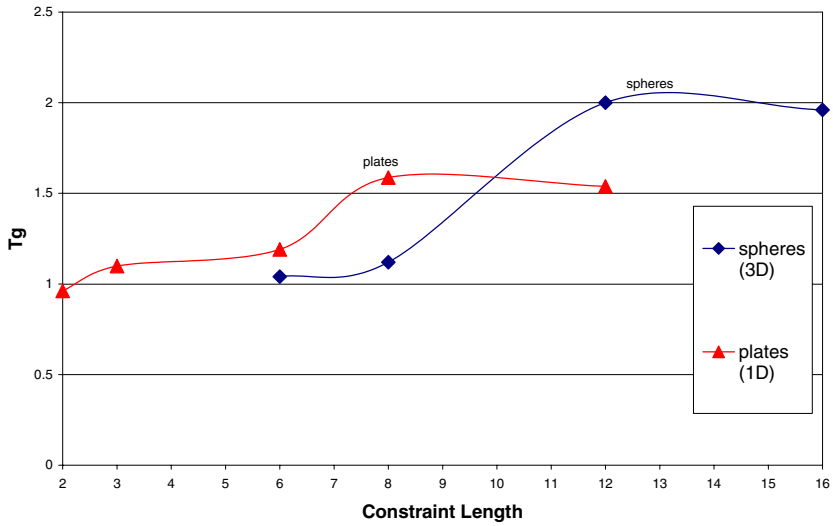

Figure 3. Variation in T_g versus constraint length in spheres and plates for $0.1x$ cooling rate.

of change in the density as the temperature was lowered. However, these runs required much more supercomputer time and therefore a higher starting density and longer chains were not deemed practical or necessary for the comparison studies listed in table 1. The data reported here were conducted on the supercomputer system of the United States' National Institute of Standards and Technology (NIST) and required several hundred hours of computer time over the past two years.

The break in the rate of change in density is indicative of a second-order liquid to glass transition. In order to characterize this transition, a 'liquid' density versus temperature, V/kT, line was drawn through overlapping density values and extended through the slowest rate of cooling values of density as shown in figure 2. Then separate lines representing the rate of

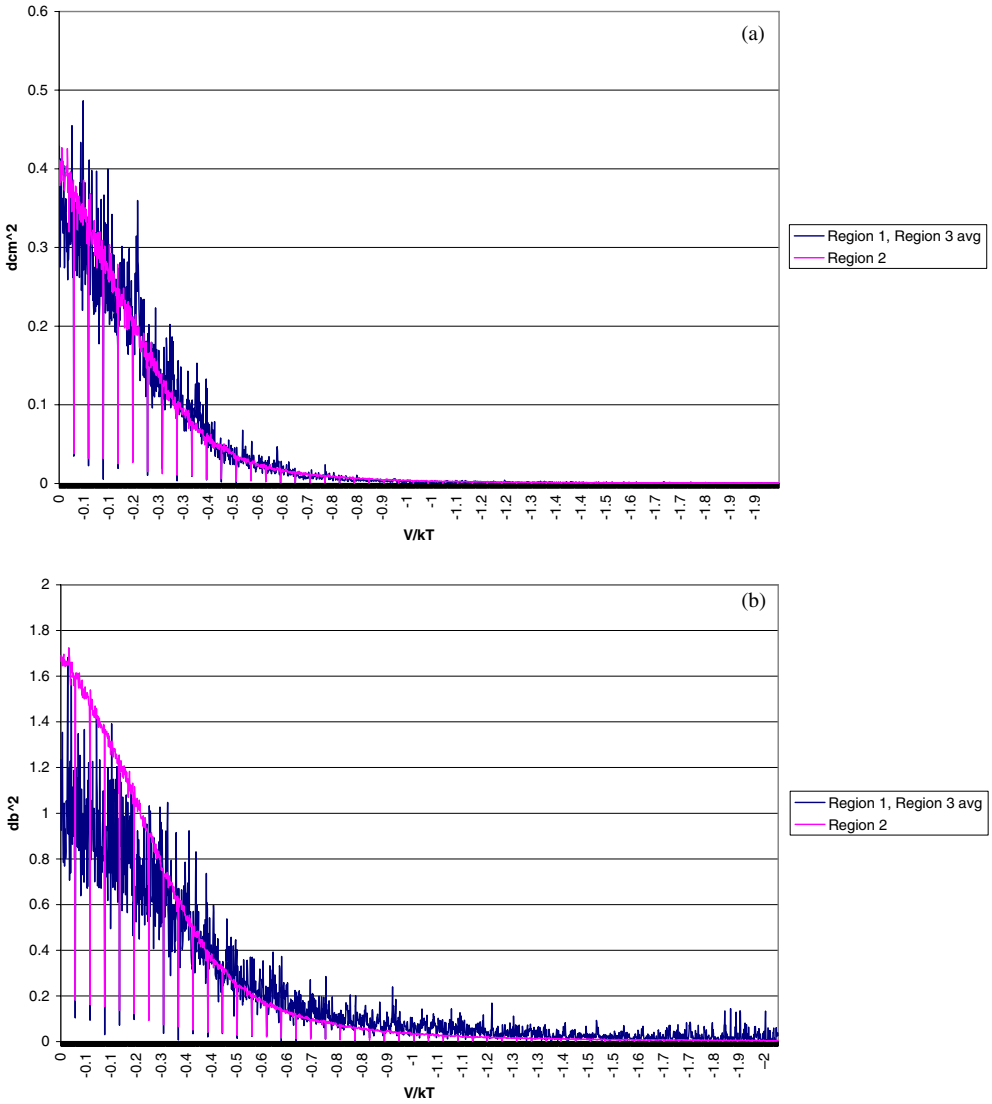

Figure 4. (a) Distance squared moved by centre of mass when confined by plates 12 units apart in a time interval of 1 Rouse relaxation time and $0.1x$ cooling rate. Regions 1 and 3 are 0–2 units from the plate wall; region 2 is 6 units wide in the centre. (b) Distance squared moved by the beads for the conditions in figure 4(a).

change in density with temperature for each cooling rate in the 'glassy' region were drawn. The intersection of the liquid line with the 'glass' rate of change in density for each cooling rate was used to determine an effective T_g for that environment and cooling rate. The change in density in the model's 'liquid' state is higher than in the hydrocarbon liquid as the density in the model is half that of the hydrocarbon. The change in density of the 'glass' is small, as expected.

The resulting values of $1/T_g$ and T_g, where V/k is set equal to 1, are reported in table 1 for each of the four 3D spherical and five 1D film constraining environments. A plot of T_g versus

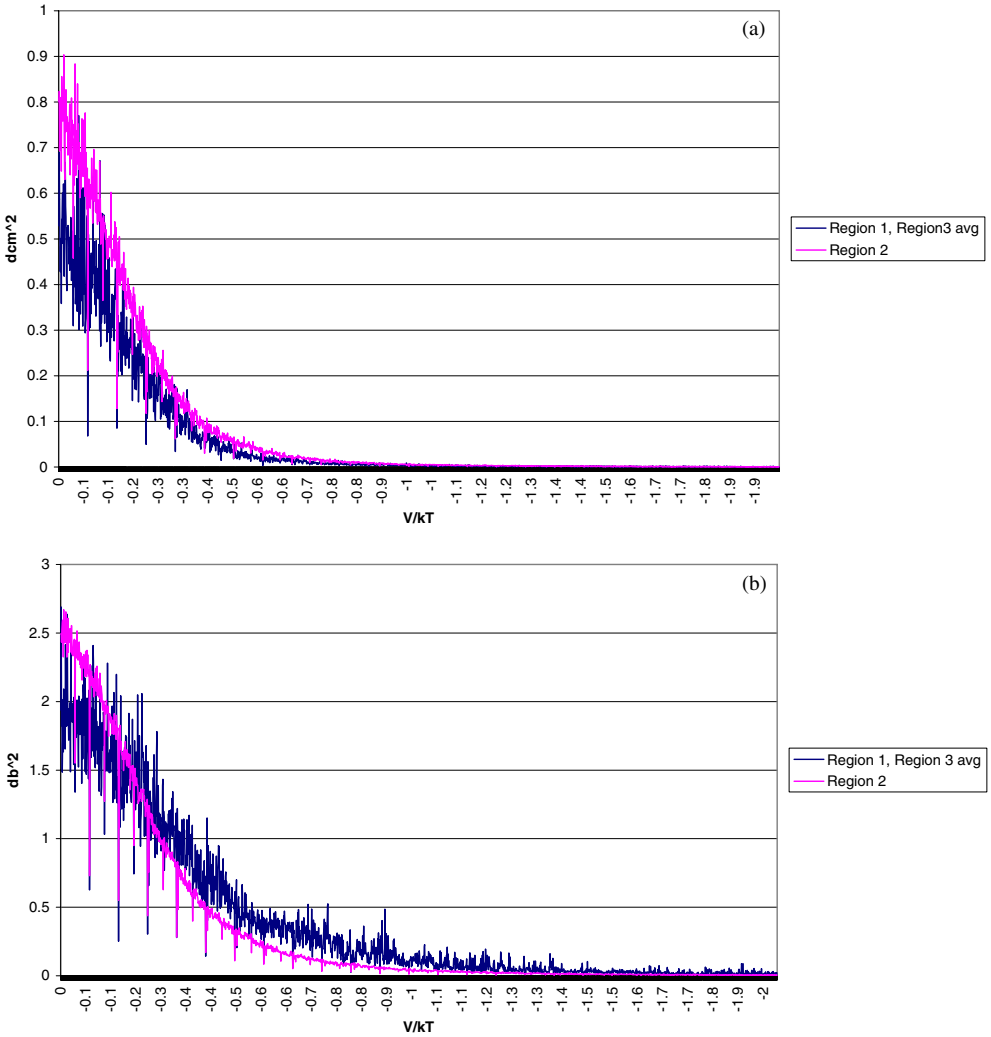

Figure 5. (a) Distance squared by centre of mass when chains are confined between 2 plates 8 units apart in a time interval of 1 Rouse relaxation time; cooling rate $0.1x$. Regions 1 and 3 are 0–2 units from plates; region 2 is 6 units wide in the centre. (b) Distance squared moved by beads for the conditions in figure 5(a).

constraint length is shown in figure 3. Figure 3 demonstrates that the effect of the confining dimension begins at a larger dimension in 3D spherical confinement than in 1D confinement between two plates. This is in agreement with previous experimental results [27]. The limiting no-confinement, large-dimension value of T_g for the 1D and 3D environments is clearly the same. For a constraint length of 16, the 1D value for T_g would be close to the 3D system with a diameter of 16. Figure 3 suggests that an ultimate limit of the effect on T_g is also independent of the confining geometry.

In order to evaluate the effect of confinement on the mobility of the polymer chains, the mean square displacement over units of time equal to one and 50 Rouse relaxation times was monitored. The distance squared per unit time was monitored for both the centre of mass of

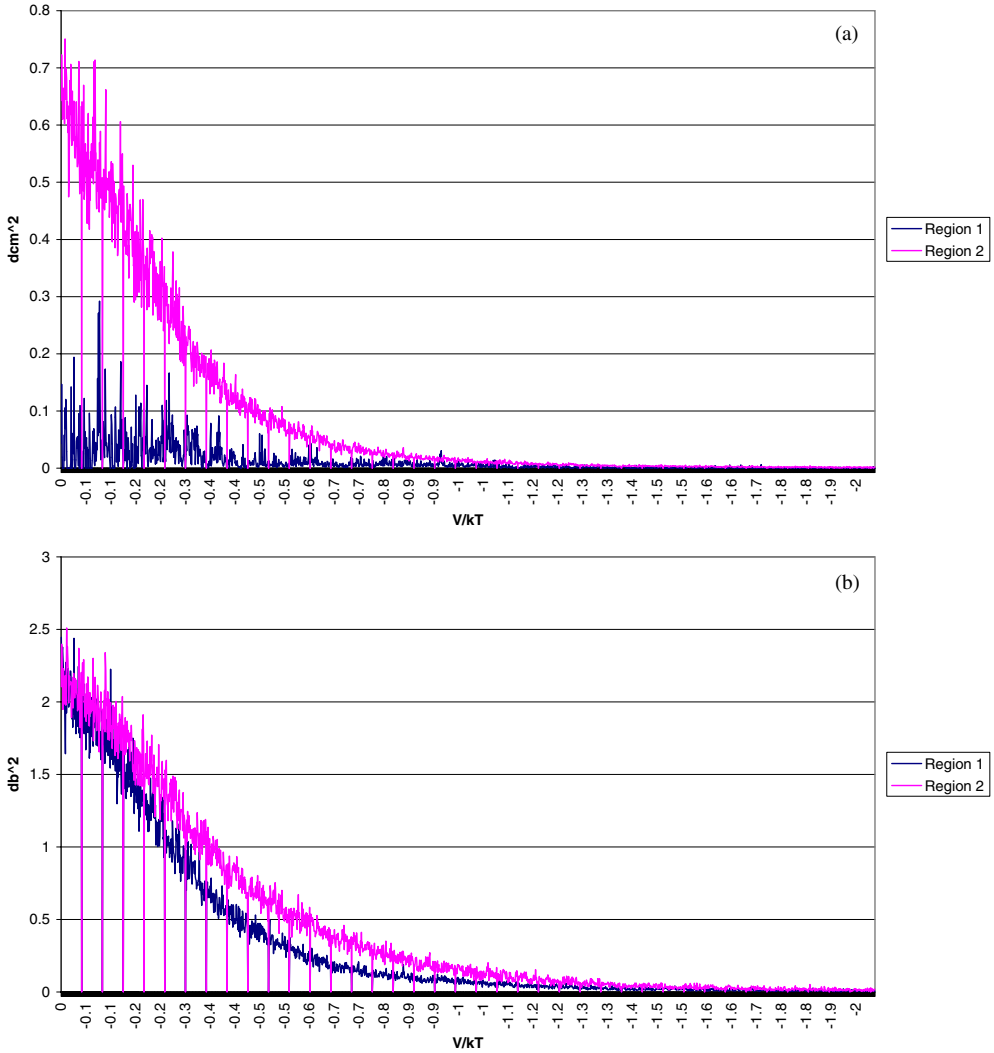

Figure 6. (a) Distance squared moved by centre of mass when chains are confined in a sphere; radius 4; cooling rate 0.1x; time interval 1 Rouse relaxation time. Region 1 is a spherical region, radius 1 in the centre and region 2 is the shell, thickness 3 between the confining walls and the spherical region in the centre. (b) Distance squared moved by individual beads for the conditions in (a).

the 10-bead chain and for the individual beads. In the 1D confinement between parallel plates and the 3D confinement in spheres, the mobility was monitored in a region near the confining wall and in the centre of the confining space.

Figures 4 and 5 report the results for confinement between parallel plates separated by distances of 12 and 8 units. The results indicate that the mobility of the beads is initially less in the region near the repulsive confining wall compared to the centre. As the temperature decreases, and the density increases, the figures suggest that the mobility near the walls approaches that of the beads further from the wall in the centre. A reason for the approach to uniform mobility is that the repulsive walls cause the chains to move away from the walls as the

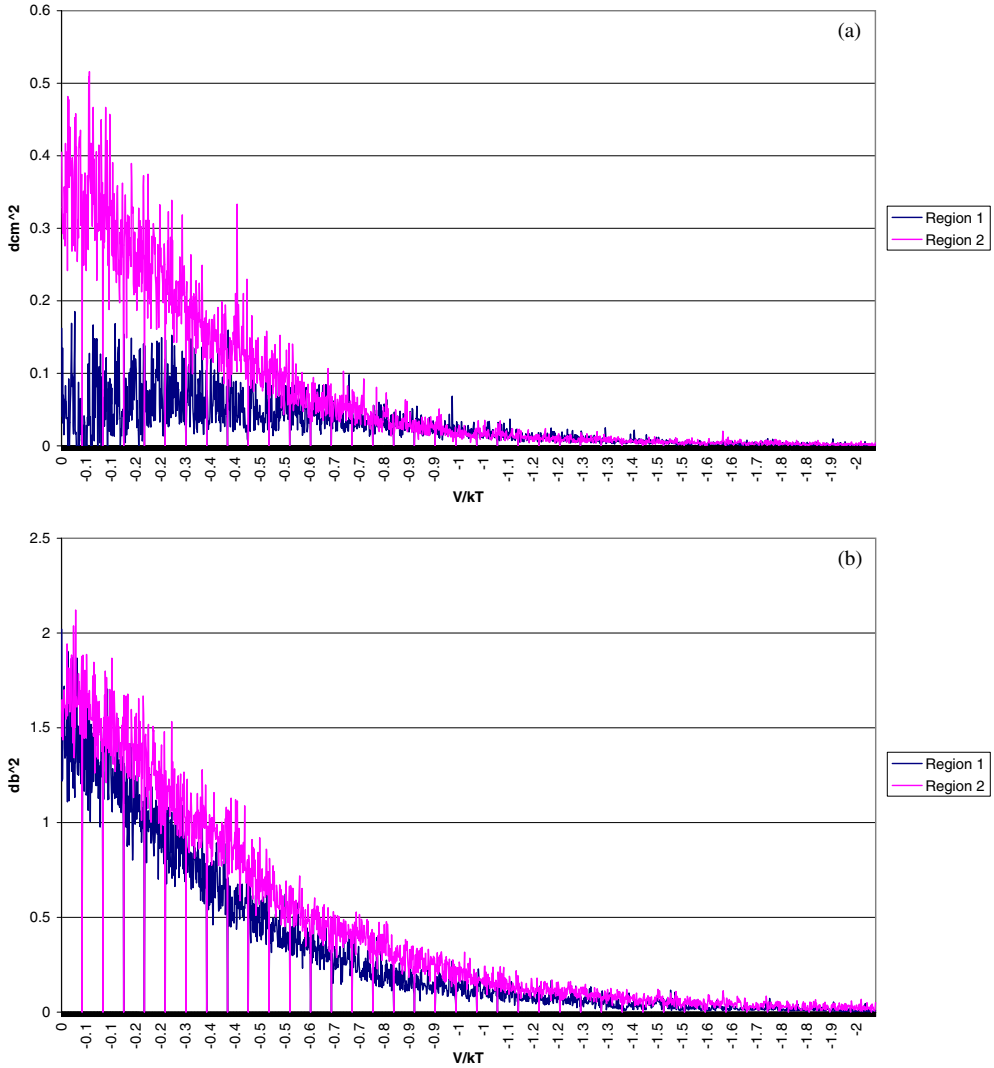

Figure 7. (a) Distance squared moved by centre of mass in a sphere, radius 3, cooling rate $0.1x$, time interval 1 Rouse relaxation time. Region 1 is a spherical region, radius 1 in the centre. Region 2 is a shell, thickness 2 between the confining walls and region 1. (b): Distance squared moved by beads for the conditions in figure 7(a).

density increases with a decrease in temperature and the resulting deepening of the attractive well as V/kT becomes more negative.

The results for spherical confinement in spheres of radius 4 and radius 3 are shown in figures 6 and 7, respectively. Here in the 3D confinement, the figures show that there is a lower mobility in the centre of sphere than in the outer region. The effect is more pronounced for the mobility of the centre of mass. The difference in mobility between these two regions persists throughout the cooling cycle. Figure 8 displays the result for the sphere of radius 6 when the mobility is monitored over intervals of 50 Rouse relaxation times. Again, a distinct difference in mobility between the centre region and the outer region is observed, with a higher mobility in the outer region due to the lower bead density in the region near the confining walls.

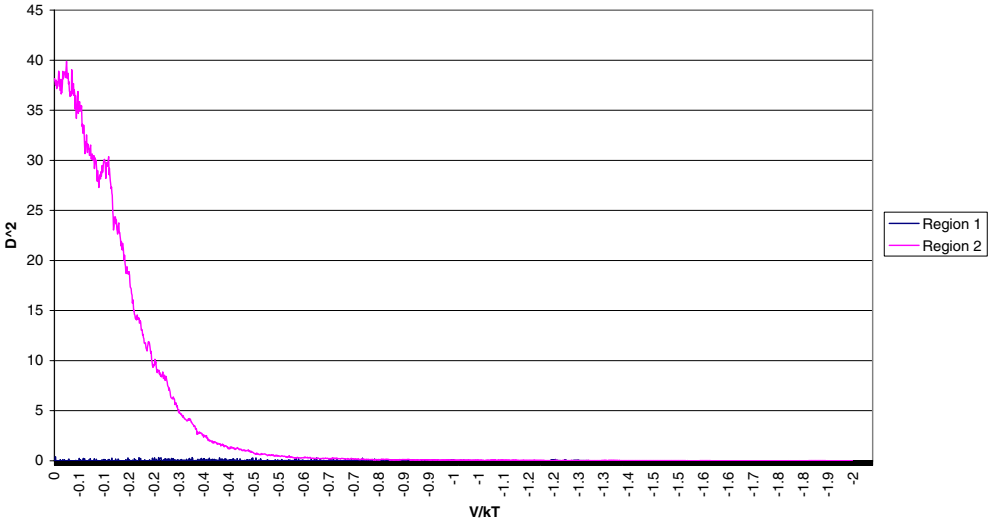

Figure 8. Distance squared moved by centre of mass for the sphere of radius 6 under the conditions in figure 6(a) but sampling interval is 50 Rouse relaxation times. Region 1 is the inner sphere of radius 2. Region 2 is the remaining outer shell of thickness 2.

4. Conclusions

Overall, the effect of a purely repulsive confining wall is to lower the glass transition temperature. Differences exist between the mobility of the beads near the confining wall and the interior of the confining region.

In the case of confinement between parallel plates, the mobility is initially less near the purely repulsive wall. As the temperature decreases, the mobility of beads in the outer region becomes equal to that in the interior. The most likely cause is the increase in density with cooling and a resulting contraction away from the repulsive wall as the attractive force between the beads increases with the decrease in temperature.

In the case of confinement with a sphere with repulsive walls, there is a higher mobility in the outer region or shell nearest the confining wall, relative to the interior. This difference in mobility persists throughout the cooling cycle. Thus, in 3D confinement there is a strong dynamic heterogeneity. Clearly, differences between confinement under purely repulsive walls in spheres versus confinement between two parallel plates include that the cooperative length scale is cut off in all three directions versus allowing two dimensions to have large scale dimensions; that the surface to volume ratio is much higher in the spheres; and that the geometry of the repulsive force in 3D confining spheres differs significantly from that in 1D confining parallel walls. The deeper physical reasons for this distinctly different result for 3D confinement compared to confinement where only one dimension is small are an open question.

Acknowledgment

The authors thank the NSF, Grant INT-0003760, for providing partial support of this work.

References

[1] Jackson C L and McKenna G B 1990 *J. Chem. Phys.* **93** 9002
[2] Jackson C L and McKenna G B 1991 *J. Non-Cryst. Solids* 221
[3] Richert R 2002 *Phy. Chem. 223 SCS Mtg* (Washington, DC: American Chemical Society) (Abstracts)
[4] Cramer C, Cramer T, Arndt M, Kremer F, Naji L and Stannarius R 1997 *Mol. Cryst. Liq. Cryst. Sci. Tech.* **303** 209
[5] Arndt M, Stannarius R, Groothues H, Hempel E and Kremer F 1997 *Phys. Rev. Lett.* **79** 2077
[6] Pissis P, Daoukako-Piammanti D, Apkis L and Christodoulides C J 1994 *J. Phys.: Condens. Matter* **6** 325
[7] Stickel F, Kremer F and Fischer E W 1993 *Physica* A **201** 318
[8] Zhang J, Liu G and Jonas J 1992 *J. Phys. Chem.* **92** 3478
[9] Schuller J, Richert R and Fischer E W 1995 *Phys. Rev.* B **52** 15232
[10] Streck C, Mel'nichenko Y and Richert R 1996 *Phys. Rev.* B **53** 15341
[11] Mel'nichenko Y, Schuler J, Richert R and Ewen B 1995 *J. Chem. Phys.* **103** 2016
[12] Gorbatschow W, Arndt M, Stannarius R and Kremer F 1996 *Europhys. Lett.* **35** 719
[13] Huwe F, Kremer F, Behrens P and Schwieger W 1999 *Phys. Rev. Lett.* **82** 2338
[14] Kremer F, Huwe A, Arndt M, Behrens P and Schwieger W 1999 *J. Phys.: Condens. Matter* **11** A175
[15] Rittig F, Huwe A, Fleischer G, Kärger J and Kremer F 1999 *Phys. Chem. Chem. Phys.* **1** 519
[16] Huwe A, Kremer F, Hartmann L, Kratzmüller T, Braun H G, Kärger J, Behrens P, Schwieger W, Ihlein G and Schüth J 2000 *J. Physique* IV **10** 59
[17] Haralampus H, Argiviadi P, Gilchriest A, Ashmore E, Scordalolees C, Martin W and Verdier P 1998 *J. Non-Cryst. Solids* **42** 235
[18] Keddie J, Jones R L and Cory R 1994 *Europhys. Lett.* **27** 59
[19] Schonhals A, Goering H and Schick C 2002 *J. Non-Cryst. Solids* **305** 140
[20] Forrest J, Dalnoki-Veress K, Stevens J and Dutcher J 1996 *Phys. Rev. Lett.* **77** 2002
[21] Forrest J and Jones R 2000 *Polymer Surfaces, Interfaces and Thin Films* ed A Karim and S Kumar (Singapore: World Scientific) p 251
[22] Forrest J, Dalnoki-Veress K and Dutcher J 1997 *Phys. Rev.* E **56** 5705
[23] deGennes P 2000 *Eur. Phys. J.* E **2** 201
[24] Hartmann L, Kratzmüller T, Braun H G and Kremer F 2000 *Macromolecules* **21** 814 (Rapid Communication)
[25] Hartmann L, Kratzmüller T, Braun H G and Kremer F 2000 *J. Physique* IV **10** 309
[26] Torres J, Nealey P and dePablo J 2000 *Phys. Rev. Lett.* **85** 3221
[27] Pelster R 1999 *Phys. Rev.* B **59** 9214
[28] Varnik F, Baschnagel J and Binder K 2000 *J. Physique* IV **10** 239
[29] Varnik F, Baschnagel J and Binder K 2000 *J. Chem. Phys.* **113** 4444
[30] Varnik F, Baschnagel J and Binder K 2002 *Phys. Rev.* E **65** 021507
[31] Mischler C, Baschnagel J and Binder K 2001 *Adv. Colloid Interface. Sci.* **94** 197
[32] Kranbuehl D, Knowles R, Hossain A and Gilchrist A 2002 *J. Non-Cryst. Solids* **307** 495
[33] Ngai L L and Rizos A K 1996 *Mater. Res. Symp. Proc.* **455** 147
[34] Kranbuehl D E, Eichinger D and Verdier P H 1991 *Macromolecules* **24** 2419
[35] Kranbuehl D E and Verdier P H 1997 *J. Chem. Phys.* **106** 4788